Role of Unidirectionality and Reverse Path Length on Wireless Sensor Network Lifetime

Anil Ufuk Batmaz, Huseyin Ugur Yildiz, and Bulent Tavli

***Abstract*—Transceiver characteristics, asymmetric interference, and various properties of electromagnetic propagation environment create unidirectional links in Wireless Sensor Networks (WSNs), especially in extreme environments. Utilization of unidirectional links is shown to improve network connectivity and lifetime. In practical WSNs, link level data exchange is performed through handshaking. However, a special handshake mechanism, where Acknowledgement (ACK) packets are conveyed through a multi-hop reverse path, is necessary to be able to utilize unidirectional links. In this mechanism, hop length of the reverse path is a key design parameter because by allowing longer reverse paths more unidirectional links can be utilized. However, increasing the reverse path hop length increases the energy overhead due to the extra ACK packets. Furthermore, complexity of maintaining the data flow also increases as the allowed maximum reverse path hop length increases. In this study, we seek the answer of the following question: What is the optimum number of hops allowed for the reverse path hop length in WSNs? We created a novel Mixed Integer Programming (MIP) framework to characterize the impact of reverse path hop length on WSN lifetime and performed extensive numerical analysis. Our results show that reverse path hop length has a significant impact on WSN lifetime.**

***Index Terms*—wireless sensor networks, unidirectional links, extreme environments, mixed integer programming, energy efficiency.**

I. Introduction

In Wireless Sensor Networks (WSNs), communication links are generally assumed to be bidirectional (*i.e.*, node pairs exchange packets in both directions) [1]. On the other hand, the link bidirectionality assumption does not hold in many practical network deployments (*i.e.*, a significant portion of links in various wireless network testbeds are shown to be unidirectional [2], [3]). Link unidirectionality is related to several physical factors (*e.g.*, transceiver characteristics and unequal interference). Transmission power heterogeneity (*i.e.*, a high transmission power node can reach a low transmission power node, however, communication in the reverse direction is not possible) [4] and random irregularities due to ambient factors affecting the signal propagation path (*e.g.*, noise, interference) [2] are salient factors that lead to link unidirectionality.

Extreme environments (*e.g.*, very high or very low temperatures) further aggravates the unidirectionality in WSNs because power amplifier characteristics of individual transceivers in a network deviate more significantly at extreme temperatures [5], [6]. Furthermore, in [7], [8], it is shown that in extreme environments (*e.g.*, environments with high levels of interference such as industrial deployments) where link reliability is low, links are prone to be unidirectional.

Most Medium Access Control (MAC) layer protocols (*e.g.*, IEEE 802.11) are designed to use bidirectional links (*e.g.*, in handshaking mechanism, data transmission by a transmitter should be replied back with an acknowledgement – ACK – transmission by the receiver). Routing protocols utilizing such MAC protocols can utilize only bidirectional links for routing [9]. However, for performance optimization reasons utilization of unidirectional links in conjunction to bidirectional links is necessary. To facilitate the use of unidirectional links many MAC protocols that have the capability to utilize unidirectional links are proposed. These protocols are designed to perform handshaking over unidirectional links (*i.e.*, ACK packets are relayed back to the transmitter in a multi-hop fashion by using one or more relay nodes) [2]. Here, an important design problem is to determine the maximum reverse path length for unidirectional links. Note that the minimum reverse path length is two hops for any unidirectional link (*i.e.*, there is only one relay node to forward the ACK packets from the receiver to the transmitter).

In literature there are a few studies on investigation of the effects of unidirectional links on network protocols [10], [11]. Furthermore, in several studies protocols that enable routing data over unidirectional links in Mobile Ad Hoc Networks (MANETs) [2], [4], [12], [13] and WSNs [9], [14] are proposed. In fact, utilization of unidirectional links necessitates a cross layer design approach because in traditional layerist approach the MAC layer does not perform any multi-hop routing functionality which is necessary for the reverse path ACK flows in unidirectional links. All solutions proposed for routing over unidirectional links are designed to incorporate multi-hop reverse path concept into the protocol architecture. Different from the existing body of work in the literature which focus on the design of protocols for unidirectional links and performance evaluations of protocols in networks with unidirectional links, we investigate the impact of reverse path length on WSN lifetime under ideal operating conditions. In our earlier work [15], we investigate the effects of unidirectionality on WSN lifetime, however, the optimization framework we developed in [15] is not capable of investigating the effects of reverse path length.

One of the most important design objectives for WSNs is lifetime optimization. To avoid premature exhaustion of any sensor node's energy dissipation should be evenly shared throughout the network which can be achieved by optimally balancing the flows. Lifetime can be maximized if both bidirectional and unidirectional links are utilized because

The authors are with TOBB University of Economics and Technology, Ankara,Turkey (e-mail: {aubatmaz, huyildiz, btavli}@etu.edu.tr).

elimination of any available link limits the options for energy balancing. However, utilization of unidirectional links are more costly than utilization of bidirectional links due to the multi-hop reverse path required for ACKs. Furthermore, the cost of unidirectional links increases as the reverse path length increases. The impact of any relevant paradigm affecting the energy dissipation characteristics of WSNs is worth investigating [16], yet, a systematic characterization of the impact of reverse path length on WSN lifetime through mathematical programming has not been performed in the literature. On the other hand, the impact of unidirectional links on other aspects of wireless networks such as network connectivity for a certain protocol has been analyzed in earlier work (*e.g.*, [2]).

The literature on mathematical programming based optimization, modeling, and analysis of WSNs is extensive and has grown rapidly in recent years. Providing a comprehensive overview of the published research on modeling WSNs through mathematical programming is beyond the scope of our work. We refer interested readers to the recent review papers on this topic [17], [18].

In this study, we investigate the impact of reverse path length of unidirectional links on WSN lifetime. We construct a novel mathematical programming framework by employing two commonly employed unidirectionality abstractions for wireless networks. By utilizing the developed models we explore a wide ranging parameter space.

The rest of the paper is organized as follows. The mathematical programming framework is elaborated in Section II. Numerical analysis to explore the parameter space and to quantify the impact of reverse path length are given in Section III. Section IV provides our concluding remarks.

II. Model

In this study, our main goal is to characterize the effects of unidirectional links induced by transmission power heterogeneity and random irregularities on network lifetime. In this section, we define our system model, clarify the assumptions, and formulate the optimization problem.

A. System Model

According to results of experiments in actual WSN testbeds energy dissipation is overwhelmed by communication energy consumption rather than computation (*e.g.*, communication energy dissipation constitutes 91% of the total energy dissipation in Telos sensor nodes [19]). Therefore, to maximize the network lifetime, the most important operation to be optimized for energy efficiency is conveying the data from sensor nodes to the sink.

We adopt a widely utilized energy dissipation model in our framework [20]. In this model, $E_{tx,ij} = \rho + \varepsilon d_{ij}^{\alpha}$ represents the amount of energy required to transmit one bit of data and $E_{rx} = \rho$, represents the amount of energy necessary to receive one bit of data, where ρ expresses the energy dissipated in the electronic circuitry, ε denotes the transmitters efficiency, α represents the path loss, and d_{ij} is the distance between node-*i* (transmitting node) and node-*j* (receiving node).

In our network model, there are N sensor nodes, including a single sink. Time is organized into rounds with equal duration T_{rnd}. Each node in the network-*i* produces the same amount of data at each round to be conveyed to the sink (*i.e.*, sensor nodes create CBR flows). Generated data at each node terminates at the sink either by direct transmission or through other sensor nodes acting as relays. The network topology is represented as a directed graph, $G = (V, A)$. V is the set consisting of all sensor nodes and the sink (node-1). Set W includes all the sensor nodes except the sink (*i.e.*, $W = V \setminus \{1\}$). The set of arcs are defined as: $A = \{(i, j) : i \in V, j \in V \setminus \{i\}\}$ which implies that no node can send data to itself. Integer variable f_{ij} represents a sensor node's total number of fixed sized data packets transmitted by node-i and received by node-j throughout the network lifetime. Data generated at node-i at each round in terms of number of data packets is denoted as s_i. Flow of ACK packets originated at node-j in reply to data flow f_{ij} is represented by integer variable g_{ji}^{kl} where node-k and node-l are the relay nodes for the ACK flow. If the link between node-i and node-j is bidirectional then $g_{ji}^{kl} \neq 0$ only for $(k, l) = (j, i)$.

We use two different unidirectionality models to create networks with unidirectional links: transmission power heterogeneity model (*D*-model) and random irregularity model (*P*-model). Most of the studies on link unidirectionality use transmission power heterogeneity (nodes have unequal transmission ranges) to create link asymmetry [2], [4], [10]–[12], [21]. In *D*-model, the nominal maximum transmission range of nodes are denoted as R_{nom}. Deviation from the nominal maximum transmission range leading to transmission power heterogeneity is modeled as a uniform random distribution in $[-R_{het}, R_{het}]$ range (*i.e.*, each node-i has a maximum transmission range of $R_{max,i} = R_{nom} + R_{dev,i}$, where $R_{dev,i}$ is an instance of random variable in $[-R_{het}, R_{het}]$ interval). Thus, node-i's maximum transmission range can, at most, be $R_{max,i} = R_{nom} + R_{het}$ and can, at least, be $R_{max,i} = R_{nom} - R_{het}$. Random irregularity model is also used to model networks with unidirectional links [2], [13], [22]. In *P*-model, N sensor nodes are randomly distributed over a predetermined network area. All sensor nodes have the same maximum transmission range (R_{nom}), thus, all node pairs with an inter-node distance lower than R_{nom} are connected via bidirectional links. By using the created bidirectional topology, each link between any connected node pair is converted to a unidirectional link with probability p_l to obtain a unidirectional network topology. Conversion to unidirectionality is achieved by randomly deleting one of the arcs between node-i to node-j (*i.e.*, either arc (i, j) or (j, i) is deleted but not both).

B. Basic Model

The base optimization problem is formulated as a Mixed Integer Programming (MIP) model, presented in Figure 1. The objective is to maximize network lifetime by finding the f_{ij}'s (data flows) and g_{ij}^{kl}'s (ACK flows) that satisfy the constraints. Note that variable T gives the network lifetime in terms of number of rounds and the actual network lifetime

can be expressed by the product $T \times T_{rnd}$. Subsection II-C presents additional constraints for incorporating transmission power heterogeneity and random irregularities induced link unidirectionality into the base MIP model.

Equation 1 and Equation 2 state that all flows are non-negative. Equation 3 is used for flow balancing at the sensor nodes. The difference of incoming flows (from other sensor) and outgoing flows (to other sensors acting as relays or to the sink) is equal to the amount of generated data at node-i. Note that $T \times s_i$ gives the total amount of data packets generated at sensor node-i (s_i is the number of fixed sized data packets generated at sensor node-i in each round which is a constant). Equation 4 guarantees that all data generated at the sensor nodes terminate at the sink. Equation 5 ensures that there are no outgoing flows from the sink. In many WSN applications sensor nodes acquire data periodically and captured data have a predetermined constant size [16], [20].

Maximize T
Subject to:

$$f_{ij} \geq 0 \ \forall (i,j) \in A \tag{1}$$

$$g_{ij}^{kl} \geq 0 \ \forall (i,j) \in A \ \forall k \in V \ \forall l \in W \tag{2}$$

$$\sum_{j \in W} f_{ji} + T s_i = \sum_{j \in V} f_{ij} \ \forall i \in W \tag{3}$$

$$\sum_{j \in W} f_{j1} - \sum_{j \in W} f_{1j} = T \sum_{i \in W} s_i \tag{4}$$

$$\sum_{j \in V} f_{1j} = 0 \tag{5}$$

$$f_{ij} = \sum_{k \in V} g_{ji}^{ki} \ \forall i \in W \ \forall j \in V \tag{6}$$

$$f_{ij} = \sum_{k \in V} g_{ji}^{jk} \ \forall i \in W \ \forall j \in V \tag{7}$$

$$\sum_{k \in V} g_{ij}^{ki} = 0 \ \forall i \in V \ \forall j \in V \tag{8}$$

$$\sum_{k \in V} g_{ij}^{jk} = 0 \ \forall i \in V \ \forall j \in V \tag{9}$$

$$\sum_{k \in V} g_{ij}^{kl} - \sum_{m \in V} g_{ij}^{lm} = 0 \ \forall i \in V \ \forall j \in V \ \forall l \in V \setminus \{i,j\} \tag{10}$$

$$\sum_{l \in V} g_{ij}^{kl} \leq M b_{ij}^{k} \ \forall i \in V \ \forall j \in V \ \forall k \in V \setminus \{j\} \tag{11}$$

$$\sum_{k \in V} b_{ij}^{k} \leq L_{RPHD} \ \forall i \in V \ \forall j \in V \tag{12}$$

$$\begin{aligned} &\sum_{j \in V} (L_{data} E_{tx,ij} + E_{PP}) f_{ij} \\ &+ \sum_{j \in V} \sum_{k \in V} \sum_{l \in V} (L_{ACK} E_{tx,ij} + E_{PP}) g_{ij}^{kl} \\ &+ \sum_{j \in W} (L_{data} E_{rx} + E_{PP}) f_{ji} \\ &+ \sum_{j \in V} \sum_{k \in V} \sum_{l \in V} (L_{ACK} E_{rx} + E_{PP}) g_{ji}^{kl} \\ &+ E_{DA} T \leq e_i \forall i \in W \end{aligned} \tag{13}$$

$$e_i = \xi \ \forall i \in W \tag{14}$$

Fig. 1: The Basic MIP framework

Equation 6 states that the total number of ACKs received at node-i for its data transmissions to node-j is equal to the total number of data packets it sent to node-j (either directly or by relaying through other sensor nodes as relays). Note that Equation 6 is used for end-to-end data and ACK flow balancing in the link layer. Equation 7 is used to equate the number of ACKs sent from node-j to its single hop neighbors destined for node-i to the number of data packets node-j receives from node-i. Equation 8 and Equation 9 prevent any ACK flows out of sender node-i and any ACK flows into destination node-j, respectively. Equation 10 is used to balance ACK flows at relay nodes. Equation 11 is used to determine the value of binary variable b_{ij}^{k} (*i.e.*, showing whether node-k is a relay for the ACK flow g_{ij}^{kl} or not). Equation 12 limits the maximum value of the reverse path hop distance (*e.g.*, $L_{RPHD} = 1$ means only bidirectional links can be used). Equation 13 states that for all nodes except the sink energy dissipation for data communication is bounded by the energy stored in batteries (e_i). Since both data and ACK flows are represented in terms of number of packets, we multiply them with L_{data} (data packet length in bits) and L_{ACK} (ACK packet length in bits), respectively, to represent the flows in terms of bits. Energy dissipation for packet processing is denoted by E_{PP} and data acquisition energy is denoted by E_{DA}. Equation 14 is used to assign equal battery energy to all sensor nodes.

Adopting a suitable definition of the lifetime in a WSN lifetime optimization problem is of utmost importance. The most commonly utilized lifetime definition in WSN lifetime optimization studies [17], [18], [23] is that the network lifetime is the duration between the time network starts operating and the time when the first sensor node in the network exhausts all its energy. If the aforementioned lifetime definition is employed naively then some of the sensor nodes can run out of their energies while the others are left with high levels of battery energy. Therefore, this definition of lifetime cannot capture the energy efficiency of a particular strategy. However, if the optimization problem is cast as a *MaXMiN* problem as we do in this study (*i.e.*, maximize the lifetime of the minimum lifetime node), then all nodes collaborate to avoid the premature death of any individual node by network-wide sharing of the data forwarding burden in a balanced fashion. Therefore, the lifetime definition we adopted in this study is a metric that sufficiently characterizes the energy efficiency.

WSNs are assumed to be consisting of stationary sensor nodes and unlike mobile networks topology changes are not frequent. Thus, topology discovery and route creation are one-time operations – for substantial amount of time (rounds/epochs) these functions are not repeated [20]. If

the network reorganization period is long enough then, the energy costs of these operations constitute a small fraction (less than 1%) of the total network energy dissipation [24]. Hence, routing overhead can be ignored in stationary WSNs without leading to significant underestimation of total energy dissipation.

C. Incorporating Unidirectionality

The basic model lacks any constraints that limit a node's transmission range (*i.e.*, any node can communicate with any other node in the network). Equation 15 is used to limit the maximum transmission range of nodes to R_{nom} (*i.e.*, any node pair separated by more than R_{nom} cannot communicate directly, however, multi-hop communication option is not blocked). Since there is neither transmission power heterogeneity (all nodes have the same transmission range) nor random irregularities ($p_l = 0.0$) there are no unidirectional links in such a network. The basic model and Equation 15 is used to model our baseline case.

$$f_{ij} = 0 \text{ if } \ R_{nom} < d_{ij} \ \forall (i,j) \in A \tag{15}$$

To model the flow of bits only on bidirectional links in *D*-model we introduce Equation 16, which states that unless both transmitter's (node-i) and receiver's (node-j) maximum transmission ranges are larger than or equal to the distance between them (d_{ij}) there cannot be any flow on arc f_{ij}. Recall that $R_{max,i}$ is in $[R_{nom} - R_{het}, R_{nom} + R_{het}]$ interval. Hence, the basic LP model presented in Figure 1 conjunction with Equation 16 models a network where only bidirectional links can be used for *D*-model.

$$f_{ij} = 0 \text{ if } \ \min(R_{max,i}, R_{max,j}) < d_{ij} \ \forall (i,j) \in A \tag{16}$$

In *P*-model, if the link from node-i to node-j is deleted (*i.e.*, removed from the set of arcs) then the flow on the reverse link is zeroed to allow flows on only bidirectional links. To model the deletion of links we define set A_d, which is the set of deleted links. The remaining set of links are denoted as A_p (*i.e.*, $A_p = A \setminus A_d$). The baseline case, which uses set A_p instead of set A, plus Equation 17 is used to model the case where only bidirectional links can be used to transfer data for *P*-model.

$$f_{ij} = 0 \text{ if} f_{ji} \in A_d \ \forall (i,j) \in A_p \tag{17}$$

Equation 18 and Equation 19 are used to model routing on both unidirectional and bidirectional links for *D*-model. Flow f_{ij} or g_{ij}^{kl} is zero if the distance between a transmitter and a receiver (d_{ij}) is larger than the maximum transmission range of node-i ($R_{max,i}$). This equation allows flow of bits between a transmitter and a receiver even if the link between them is unidirectional ($R_{max,i} \geq d_{ij}$ and $R_{max,j} < d_{ij}$). The basic model plus Equation 18 and Equation 19 extends our model to networks using both bidirectional and unidirectional links.

$$f_{ij} = 0 \text{ if } \ R_{max,i} < d_{ij} \ \forall (i,j) \in A \tag{18}$$

$$g_{ij}^{kl} = 0 \text{ if } \ R_{max,k} < d_{kl} \ \forall i \in V \ \forall j \in V \setminus \{i\} \ \forall k \in V \ \forall l \in V \setminus \{k\} \tag{19}$$

For *P*-model, modeling the utilization of both unidirectional and bidirectional links is achieved by using the baseline case only, however, set A is replaced by set A_p. In other words, if a link exists then existence of a flow on that link is not blocked provided that a reverse path can be found without violating Equation 12. All system variables with their acronyms and descriptions are presented in Table I.

TABLE I: Variables and their descriptions.

Variable	Description
T	Network lifetime in terms of rounds
N	Number of nodes
f_{ij}	Data flow from node-i to node-j (in terms of number of packets - integer variable)
g_{ij}^{kl}	ACK flow from node-i to node-j transmitted by node-k and received by node-l (in terms of number of ACK packets - integer variable)
b_{ij}^{k}	ACK flow indicator which is unity if node-k is a relay node for ACK flow g_{ij}^{kl} (binary variable)
M	A large integer
L_{data}	Data packet size (bits)
L_{ACK}	ACK packet size (bits)
s_i	Amount of data generated at each round by node-i (in terms of number of packets)
E_{rx}	Energy consumption for receiving one bit of data (J/bit)
$E_{tx,ij}$	Energy consumption for transmitting one bit of data from node-i to node-j (J/bit)
E_{DA}	Energy consumption for data acquisition (J)
E_{PP}	Energy consumption for packet processing (J)
d_{ij}	Distance between node-i and node-j (m)
ρ	Energy dissipated in the electronic circuitry (J/bit)
ε	Transmitters efficiency (J/bit/m^2)
α	Path loss exponent
e_i	Energy stored at each sensor node (J)
ξ	Battery energy (J)
$G = (V, A)$	Directed graph that represents network topology
V	Set of nodes, including the sink as node-1
W	Set of nodes except the sink (node-1)
A	Set of arcs (links)
A_d	Set of deleted links
A_p	Set of links remaining after deletion
T_{rnd}	Duration of one round (seconds)
R_{nom}	Nominal maximum transmission range (m)
R_{het}	Maximum deviation from R_{nom} (m)
$R_{max,i}$	Actual maximum transmission range of node-i (m)
$R_{dev,i}$	Deviation of node-i's actual maximum transmission range from the nominal maximum transmission range (m)
p_l	Link unidirectionality probability
L_{RPHD}	Maximum value of reverse path hop distance
η	Mean of a Gaussian random variable
σ	Standard deviation of a Gaussian random variable
p_{ij}^{s}	Probability of a successful data packet reception
λ_{ij}	Average number of retransmissions

III. Analysis

We use General Algebraic Modeling System (GAMS) [25] for the numerical analysis of the developed MIP model. In our analysis, each sensor node generates one data packet per round ($s_i = 1$) to be conveyed to the sink. Data and ACK packet sizes are 256 Bytes and 20 Bytes, respectively ($L_{data} = 2048$ bits and $L_{ACK} = 160$ bits). The communication parameters are chosen as $\varepsilon = 100$ pJ/bit/m^2 and $\rho = 50$ nJ/bit (same as the ones in [20]). Each node is assumed to be equipped with two AA batteries ($\xi = 25.0$ KJ). Energy consumption for data acquisition and packet processing are chosen as $600\mu J$ and $120\mu J$ [19], [26]. In Subsections III-A and III-B, $\alpha = 2$ and Bit Error Rate (BER) is taken as zero. In Subsection III-C, we modeled a harsher channel where $\alpha = 3$ and BER is non-zero.

A. Understanding the Network Dynamics

To illustrate the effects of limiting the maximum value of the reverse path length, graphically, we solve the optimization problem for the small scale topology ($N = 5$) presented in Figure 2. Figure 2a and Figure 2b present the available links for *D*-model and *P*-model, respectively. In Figure 2a, the link between node-1 and node4 is unidirectional (node-4 can reach node-1 but node-1 cannot reach node-4) due to the transmission power heterogeneity. Furthermore, the link between node-1 and node-2 is also unidirectional (node-2 can reach node-1 but node-1 cannot reach node-2). Likewise, in Figure 2b, the link between node-1 and node-3 as well as the link between node-3 and node-4 are unidirectional. Optimal flows when there are no unidirectional links in the network (*i.e.*, $R_{het} = 0$ and $p_l = 0.0$) are illustrated in Figure 2g. Network lifetimes (LT) shown in the second and third rows are normalized lifetimes obtained by dividing the lifetime values for each configuration by the network lifetime obtained for Figure 2g. In the second, third, and fourth rows of the figure solid lines are used to plot data flows and dashed lines are used to plot ACK flows.

Network lifetimes obtained for configurations with transmission power heterogeneity ($R_{het} = 125$ m) are 0.57 and 0.93 for $L_{RPHD} = 1$ (Figure 2c) and $L_{RPHD} = 2$ (Figure 2e), respectively. Figure 2d and Figure 2f present the optimal flows obtained with *P*-model ($p_l = 0.2$) for $L_{RPHD} = 1$ (LT=0.51) and $L_{RPHD} = 2$ (LT=0.75), respectively. Network lifetimes obtained for $L_{RPHD} \geq 2$ are the same with the network lifetime obtained with $L_{RPHD} = 2$ for both *D*-model and *P*-model in this scenario. In fact, neither for *D*-model (Figure 2a) nor for *P*-model (Figure 2b), there is no need to use a reverse path which is more than two hops longer in these topologies. In Figure 2a, node-1 can send ACKs to either node-2 or node-4 via node-3 in two hops. In Figure 2b, node-2 can send ACKs to node-4 via node-3 by using a two hop reverse path. Furthermore, node-3 do not need to send any ACKs to node-1 because the sink which is node-1 does not send any data packets to any sensor node.

Figure 2c and Figure 2d present the optimal flows when only bidirectional links are allowed to be used (*i.e.*, $L_{RPHD} = 1$ dictates that ACK packets can be send only directly to the transmitter by the receiver) for *D*-model and *P*-model, respectively. When compared to the case without unidirectional links (Figure 2g), network lifetime values for both cases that use only bidirectional links decrease significantly because some of the links that are vital for energy balancing are no more available (*i.e.*, they are not bidirectional). For example, in Figure 2c node-3 is the only node that is connected to the sink (node-1) and it carries all the data generated by other sensor nodes in addition to its own generated data which makes node-3 the hot spot in the network (*i.e.*, network lifetime is determined by node-3 because upon the death of node-3 there is no connection left between the sink and the rest of the network). In Figure 2d, node-3 cannot transmit data directly to the sink due to the unidirectionality of the link between node-1 and node-3. Most of the data generated in the network is transmitted to the sink by node-4 (2.75 units) and a small fraction of data is transmitted by node-3 to the sink (0.25 units).

Figure 2e and Figure 2f present the flows for *D*-model and *P*-model with $L_{RPHD} = 2$, respectively. Utilization of unidirectional links allows the network to balance the energy dissipation efficiently and improves the network lifetime significantly (*i.e.*, by increasing L_{RPHD} from one to two LT increased 63 % and 47 % for *D*-model and *P*-model, respectively). The improvement in lifetime is higher for *D*-model than *P*-model because all three sensor nodes can transmit data directly to the sink in Figure 2e (*i.e.*, for $L_{RPHD} = 1$, node-3 carries the burden of relaying the data of all the other senor nodes by itself which makes node-3 the bottleneck, however, for $L_{RPHD} = 2$, the burden of relaying is shared by all sensor nodes and premature death of node-3 is avoided), however, in Figure 2f only two of the sensor nodes can transmit directly to the sink (node-2 and node-4).

Figure 2 clearly presents the importance of L_{RPHD}. Indeed, as L_{RPHD} gets longer, more links become usable and network lifetime increases. However, is there a limit to this increase? We seek the answer to this question in Subsection III-B by exploring a larger parameter space.

B. Exploring the Parameter Space

To analyze the effect of reverse path length on network lifetime for larger topologies, we used a disc shaped network topology with a sink at the center. We use the best known disk packing geometries reported in [27] to form the constellation for N nodes in a 1000 m diameter disk.

Figure 3 and Figure 4 present the normalized network lifetimes for *D*-model and *P*-model, respectively, with $L_{RPHD} = 1$ (left column) and $L_{RPHD} = 2$ (right column) for different values of N, R_{nom}, R_{het}, and p_l. Normalization is achieved by dividing all network lifetime values of each configuration with the lifetime obtained with $L_{RPHD} \to \infty$ for the corresponding configuration. Variation of N is used to analyze the effects of node density. Since the network area is kept constant increasing N results in denser topologies. The average number of nodes and links are varied by using R_{nom}. The level of unidirectionality is investigated by varying R_{het} and p_l. The MIP problem is solved for 20 randomly selected maximum

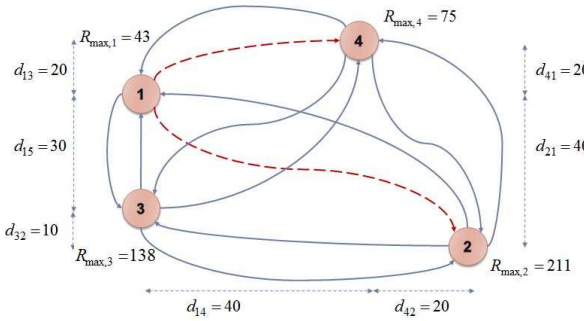

(a) $R_{nom} = R_{het} = 125$, flow=0 (dashed line), flow≥0 (solid)

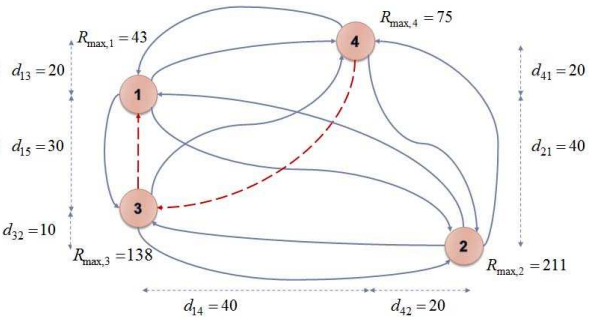

(b) $R_{nom} = 125$, $p_l = 0.2$, flow=0 (dashed line), flow≥0 (solid)

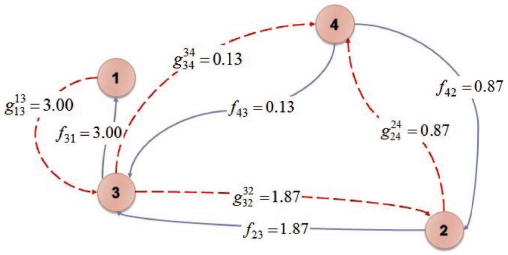

(c) $R_{nom} = R_{het} = 125$, $L_{RPHD} = 1$, *LT*=0.57

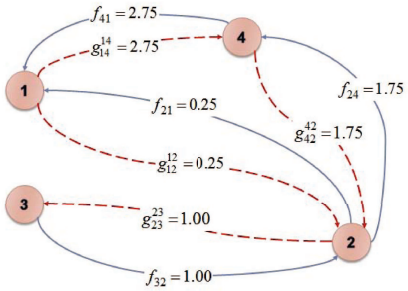

(d) $R_{nom} = 125$, $p_l = 0.2$, $L_{RPHD} = 1$, *LT*=0.51

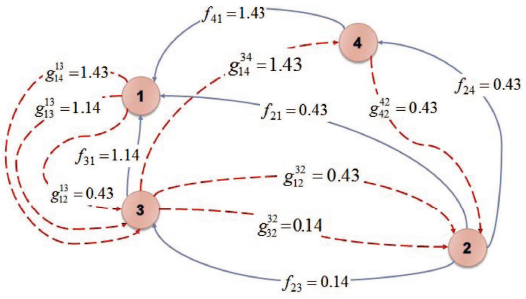

(e) $R_{nom} = R_{het} = 125$, $L_{RPHD} = 2$, *LT*=0.93

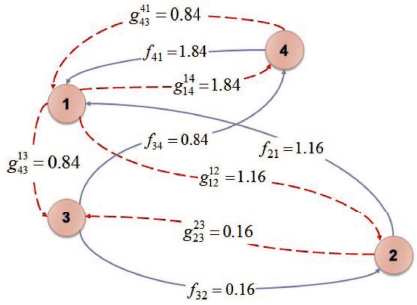

(f) $R_{nom} = 125$, $p_l = 0.2$, $L_{RPHD} = 2$, *LT*=0.75

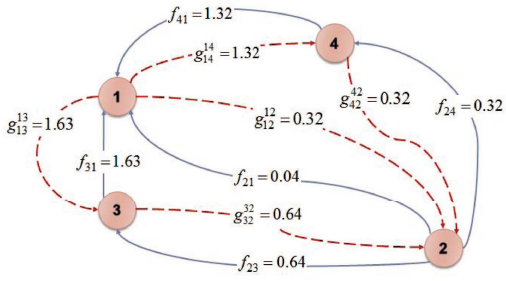

(g) $R_{nom} = 125$, $R_{het} = 0$, $p_l = 0.0$, $L_{RPHD} = 1$, *LT*=1.00

Fig. 2: Illustration of optimal routes for maximal lifetime using the parameter sets indicated. For each relevant configuration the amount of data generated by sensor nodes are normalized to unity and the numbers on each arc shows the amount of data flow. The sink is designated as node-1. Figure 2a and Figure 2b illustrate the network topologies for *D*-model and *P*-model, respectively, where usable links and unusable lines are shown by solid lines and dashed lines, respectively. Lifetimes (LT) values are normalized with the lifetime obtained in Figure 2g (the same topology without any unidirectional links).

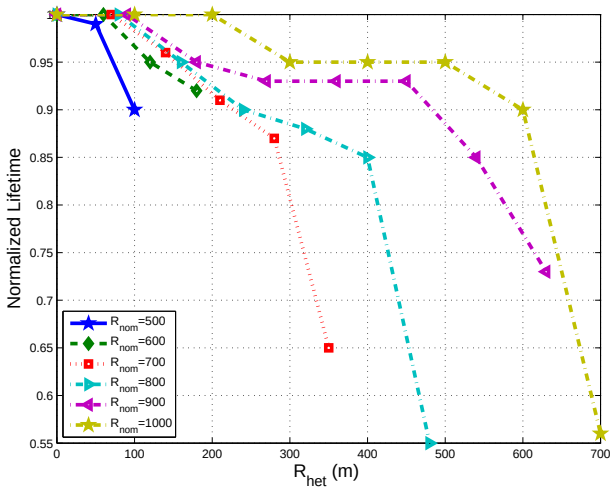

(a) $N = 20$ $L_{RPHD} = 1$

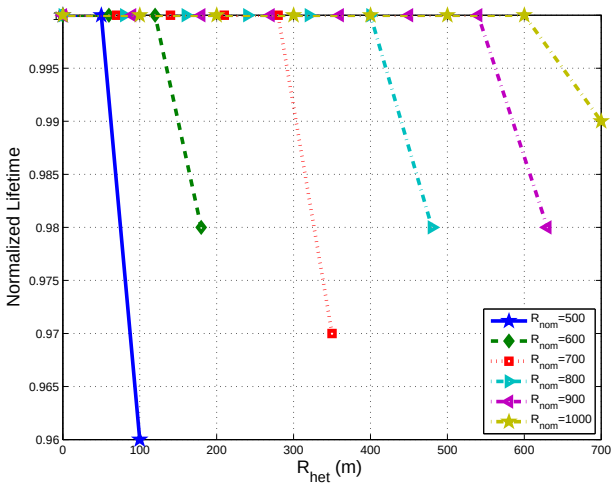

(b) $N = 20$ $L_{RPHD} = 2$

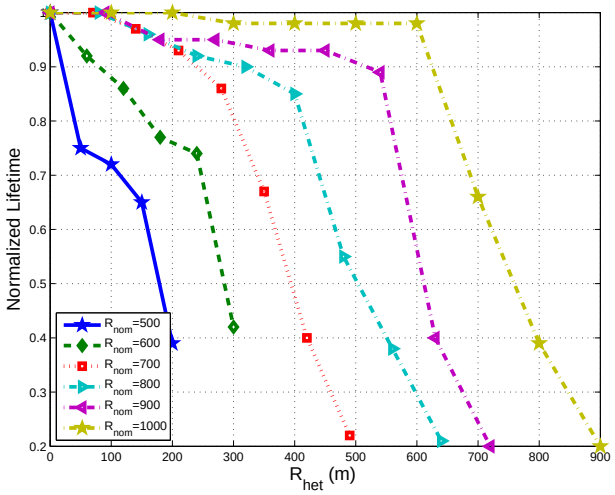

(c) $N = 25$ $L_{RPHD} = 1$

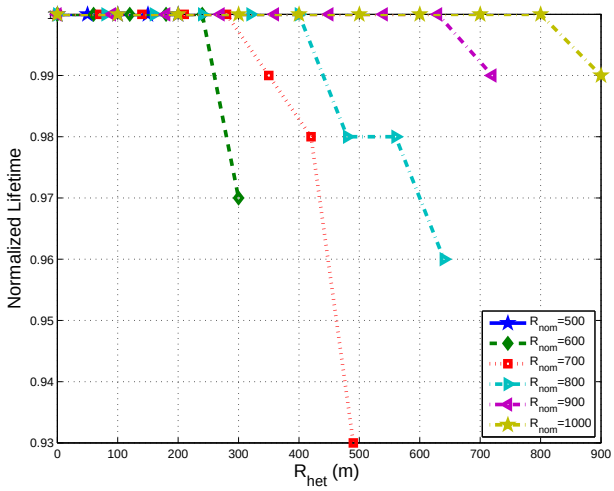

(d) $N = 25$ $L_{RPHD} = 2$

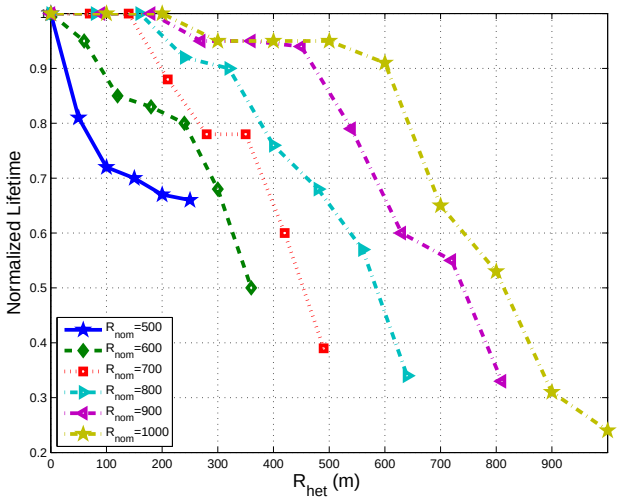

(e) $N = 30$ $L_{RPHD} = 1$

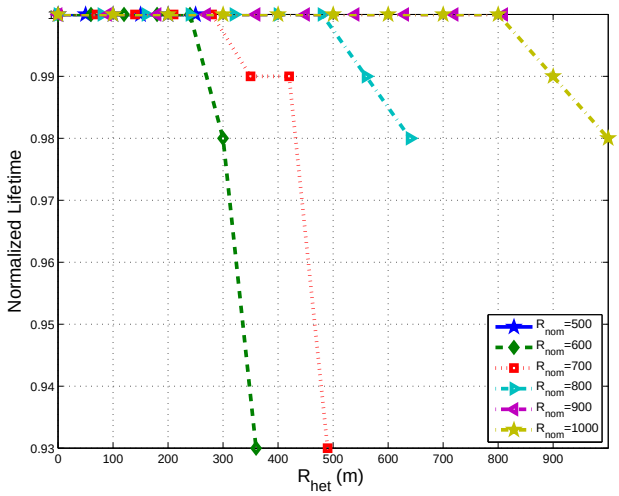

(f) $N = 30$ $L_{RPHD} = 2$

Fig. 3: Normalized lifetime in *D*-Model with $L_{RPHD} = 1$ (left column) and $L_{RPHD} = 2$ (right column) as functions of R_{het}.

transmission ranges and p_l for each node and we present the average results in the figures.

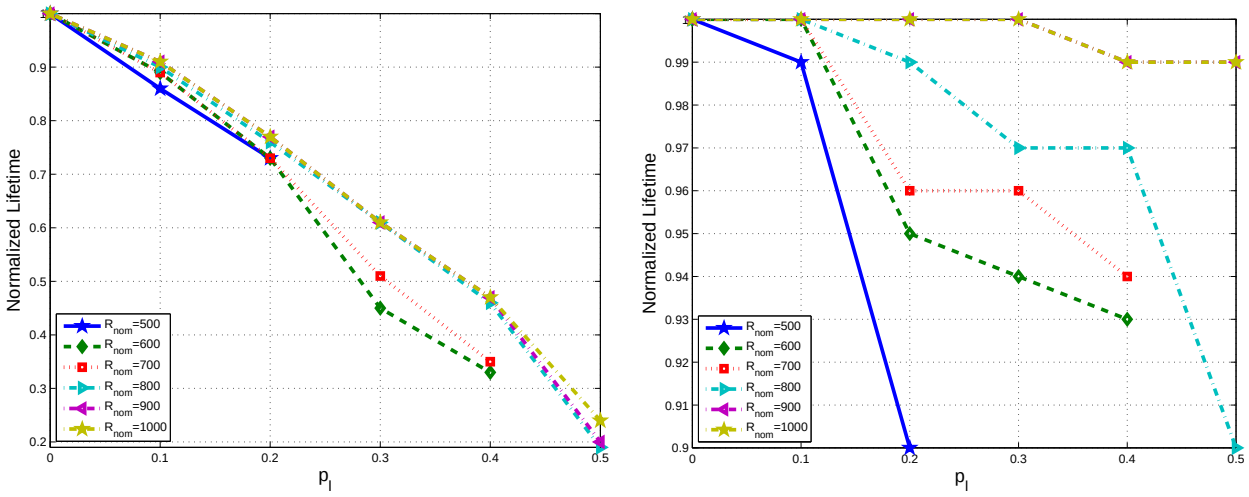

(a) $N = 20$ $L_{RPHD} = 1$ (b) $N = 20$ $L_{RPHD} = 2$

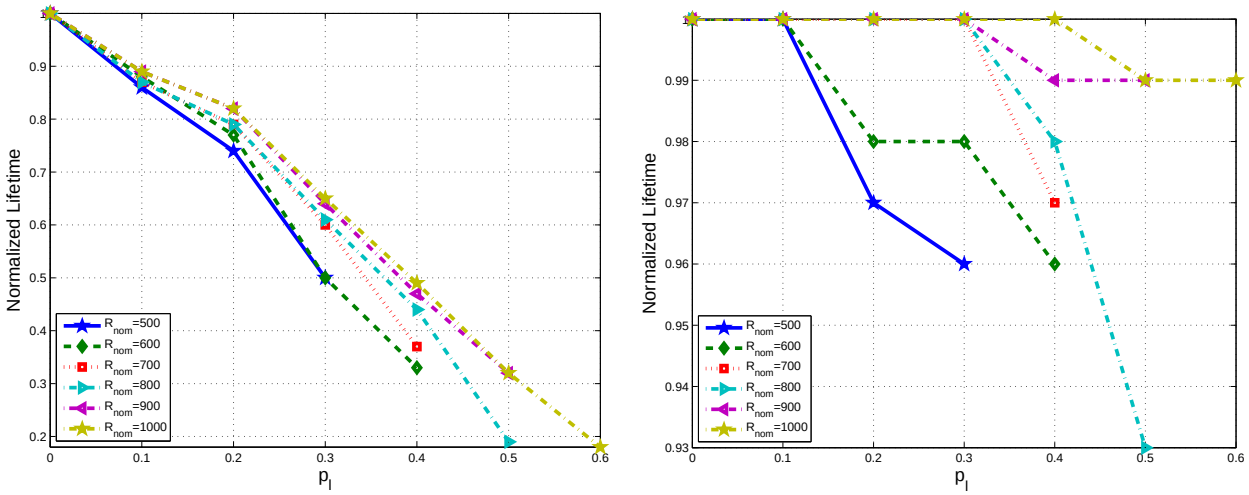

(c) $N = 25$ $L_{RPHD} = 1$ (d) $N = 25$ $L_{RPHD} = 2$

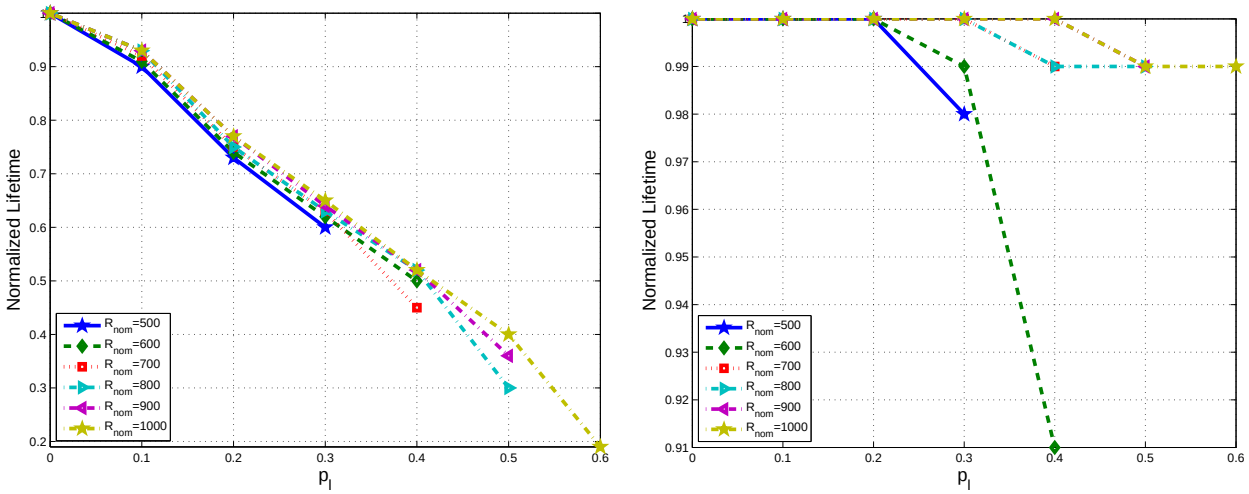

(e) $N = 30$ $L_{RPHD} = 1$ (f) $N = 30$ $L_{RPHD} = 2$

Fig. 4: Normalized lifetime in *P*-Model with $L_{RPHD} = 1$ (left column) and $L_{RPHD} = 2$ (right column) as functions of p_l.

Lifetime values cannot be presented for the whole range of R_{het} or p_l because for larger values of R_{het}/R_{nom} or

p_l we cannot get any connected topologies. A network is disconnected if at least one sensor node does not have any paths to the sink. For example, if $N = 20$ and $R_{nom} = 800$ m (Figure 3a and Figure 3b) then all topologies are disconnected for $R_{het} > 480$ m (both for $L_{RPHD} = 1$ and $L_{RPHD} = 2$). If $N = 25$ and $R_{nom} = 500$ m (Figure 4c and Figure 4d) then all topologies are disconnected for $p_l > 0.3$ (both for $L_{RPHD} = 1$ and $L_{RPHD} = 2$). We do not present lifetime results for $L_{RPHD} \geq 3$ because in any of the configurations we investigate lifetime values obtained for the same configuration do not exhibit any difference provided that $L_{RPHD} \geq 3$.

As the level of transmission power heterogeneity increases, normalized network lifetime decreases for both $L_{RPHD} = 1$ and $L_{RPHD} = 2$ as a general trend. For example, normalized network lifetime values with $N = 30$, $R_{nom} = 900$ m, and $L_{RPHD} = 1$ are 1.0 and 0.33 for $R_{het} = 180$ m and $R_{het} = 810$ m, respectively (Figure 3e). Likewise, increasing p_l leads to a decrease in network lifetime. For example, normalized network lifetime values with $N = 25$, $R_{nom} = 800$ m, and $L_{RPHD} = 2$ are 1.0 and 0.93 for $p_l = 0.1$ and $p_l = 0.5$, respectively (Figure 4d). For $L_{RPHD} = 1$ (only bidirectional links can be employed), exclusion of unidirectional links prevents the network from reaching the maximal lifetime possible with inclusion of unidirectional links especially for high unidirectionality levels. For $L_{RPHD} = 2$ (unidirectional links with at most one relay node in the reverse path can be employed in addition to bidirectional links), still some of the available unidirectional links for energy balancing cannot be utilized, therefore, the full potential of the employment of unidirectional links cannot be realized with $L_{RPHD} = 2$, especially in networks with large number of unidirectional links.

For both *D*-model and *P*-model, the lowest normalized network lifetime values obtained with $L_{RPHD} = 1$ are approximately one fifth of the $L_{RPHD} \rightarrow \infty$ case. The lowest normalized network lifetime obtained for *D*-model with $L_{RPHD} = 1$ is 0.20 which is obtained with $N = 25$, $R_{nom} = 900$ m, and $R_{het} = 720$ m (Figure 3c). For *P*-model the lowest normalized network lifetime with $L_{RPHD} = 1$ (0.18) is obtained at $N = 25$, $R_{nom} = 1000$ m, and $p_l = 0.6$ (Figure 4c). However, provided that the level of heterogeneity is low (*i.e.*, $R_{het} \leq 0.1 R_{nom}$), normalized network lifetimes values are larger than 0.75 for *D*-model with $L_{RPHD} = 1$. When the unidirectional links with only one relay node in the reverse path are allowed to be used (*i.e.*, $L_{RPHD} = 1$) the largest decrease in network lifetime is limited by at most 10 %. The lowest normalized network lifetimes for *D*-model and *P*-model are 0.93 ($N = 30$, $R_{nom} = 700$ m, and $R_{het} = 490$ m – Figure 3f) and 0.90 ($N = 20$, $R_{nom} = 500$ m, and $p_l = 0.2$ – Figure 4b), respectively. Furthermore, the decrease in normalized network lifetime is limited by 1.0 % for $p_l \leq 0.1$.

As R_{nom} gets larger, normalized network lifetime is less affected from link unidirectionality. For example, normalized network lifetime values obtained with $N = 25$, $R_{het} = 200$ m and $L_{RPHD} = 1$ (Figure 3c) are 0.39 and 1.00 for $R_{nom} = 500$ m and $R_{nom} = 1000$ m, respectively. Furthermore, with $N = 30$, $R_{het} = 360$ m and $L_{RPHD} = 2$ (Figure 4f) normalized network lifetime values are 0.93 and 1.00 for $R_{nom} = 600$ m and $R_{nom} = 900$ m, respectively. A similar trend is also observed with p_l (*i.e.*, normalized network lifetime is less affected from unidirectionality for larger R_{nom}). For example, normalized network lifetime for $N = 20$, $p_l = 0.4$, $R_{nom} = 600$ m, and $L_{RPHD} = 1$ (0.33) is higher than the normalized network lifetime obtained for $N = 20$, $p_l = 0.4$, $R_{nom} = 800$ m, and $L_{RPHD} = 1$ (0.46) as presented in Figure 4a. Normalized network lifetimes with $L_{RPHD} = 2$ with *P*-model also exhibit the same behavior (*e.g.*, for $N = 25$, $p_l = 0.3$ normalized network lifetimes values obtained with $R_{nom} = 500$ m and $R_{nom} = 800$ m are 0.96 and 1.00, respectively – Figure 4d). The reason for such behavior is that as the nominal transmission range gets larger the number of neighbors also gets larger, therefore, the reduction in the number of available links due to the same level of unidirectionality is less significant for larger nominal transmission range configurations.

C. The Impact of Packet Failures

In the previous subsections, we assumed that the BER is zero, however, it is important to investigate the effects of varying the path loss exponent (α) and non-zero BER on WSN lifetime and reverse path hop length. In this subsection, we use $\alpha = 3$ to model a fading environment. We also randomly assign BER values to each link in the network (γ_{ij}). BER is modeled as a Gaussian random variable, $N(\eta, \sigma)$, where η and σ are the mean and the standard deviation, respectively. We used five η values: 10^{-3}, 5×10^{-3}, 10^{-4}, 5×10^{-4}, and 10^{-5}. Standard deviations are chosen as one tenth of the mean values ($\sigma = 0.1\eta$).

The MIP framework presented in Section II, should be extended to model the effects of BER. We assume an ARQ (Automatic Repeat Request) mechanism is in effect which enables the retransmission of failed data packets until the packets successfully received by the intended recipients. Since we already are considering ACK packet transmissions, modeling the energy cost of this operation can be achieved by modifying the energy balance equation.

The probability of a successful data packet reception (p_{ij}^s) with a length of L_{DATA} Bytes over the link from node-i to node-j is given as

$$p_{ij}^s = (1 - \gamma_{ij})^{8 \times L_{data}}. \tag{20}$$

The average number of retransmissions (λ_{ij}) for a data packet to successfully received by the receiver on the link from node-i to node-j is

$$\lambda_{ij} = \frac{1}{p_{ij}^s}. \tag{21}$$

To account for the extra energy dissipation due to retransmissions the energy balance equation (Equation 13) should be

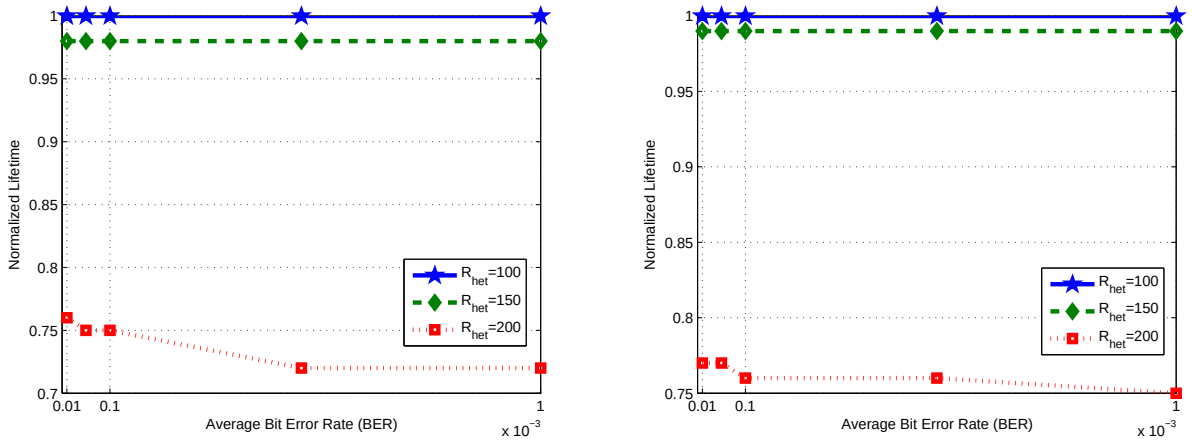

(a) $L_{RPHD} = 1$ (b) $L_{RPHD} = 2$

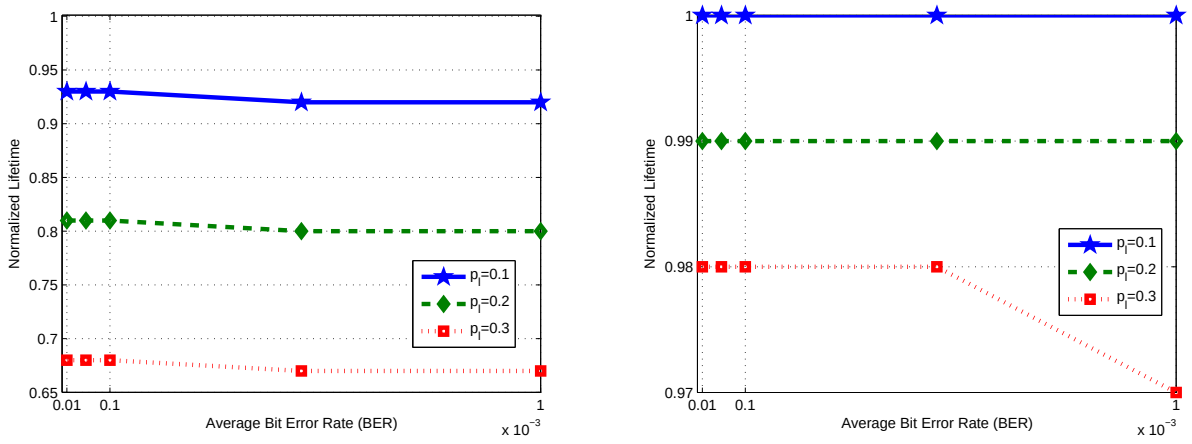

(c) $L_{RPHD} = 1$ (d) $L_{RPHD} = 2$

Fig. 5: Normalized lifetime in *D*-Model and in *P*-Model with $L_{RPHD} = 1$ (left column) and $L_{RPHD} = 2$ (right column) as functions average bit error rate per link when $N = 25$ and $\alpha = 3$.

revised as

$$\sum_{j\in V}\lambda_{ij}(L_{data}E_{tx,ij}+E_{PP})f_{ij} + \sum_{j\in V}\sum_{k\in V}\sum_{l\in V}(L_{ACK}E_{tx,ij}+E_{PP})g_{ij}^{kl} + \sum_{j\in W}\lambda_{ji}(L_{data}E_{rx}+E_{PP})f_{ji} + \sum_{j\in V}\sum_{k\in V}\sum_{l\in V}(L_{ACK}E_{rx}+E_{PP})g_{ji}^{kl} + E_{DA}T \le e_i \quad \forall i \in W. \tag{22}$$

By replacing Equation 13 with Equation 22, the MIP framework presented in Section II is employed to investigate the effects of BER.

In Figure 5, we present normalized network lifetime values as functions of p_l, R_{het}, and BER for both *D*-model and *P*-model. Nominal transmission range, network radius, and number of nodes are $R_{nom} = 500$ m, $R_{net} = 850$ m, and $N = 25$, respectively. In *D*-model, for large heterogeneity levels ($R_{het} = 200$ m), network lifetime values decrease as the BER increases for both $L_{RPHD} = 1$ (Figure 5a) and $L_{RPHD} = 2$ (Figure 5b). For example, normalized network lifetime values with $R_{het} = 200$ m and $L_{RPHD} = 1$ are 0.75 and 0.71 for $\eta = 10^{-5}$ and $\eta = 10^{-3}$, respectively. However, for $L_{RPHD} \ge 3$, all the normalized lifetime values are unity. Likewise, in *P*-model, normalized network lifetime values decrease with increasing BER values, however, for $L_{RPHD} \ge 3$ the difference between the lifetimes with different L_{RPHD} is zero. The reason for such behavior is that the network can balance the flows and achieves the maximum lifetime as long as the nodes are allowed to utilize, at most, two relay nodes in their reverse paths.

IV. Conclusion

In this study, we investigate the effects of reverse path length, required for ACK flows when utilizing unidirectional links, on WSN lifetime through a novel MIP framework. We utilize two well known mechanisms that create unidirectional links in wireless sensor networks which are transmission

power heterogeneity (*D*-model) and random irregularities (*P*-model). We explore the parameter space consisting of node density, nominal transmission range, transmission power heterogeneity level, random link disconnection probability, Bit Error Rate, and reverse path hop length (L_{RPHD}). Our results show that if the reverse path length is limited by one (*i.e.*, only bidirectional links can be used) then the network lifetime can be as low as one fifths of the lifetime obtained without any restrictions on the reverse path length. However, when the reverse path hop length is allowed to be two (*i.e.*, both bidirectional links and unidirectional links with only one node in the reverse path are can be utilized), the reduction in network lifetime is at most 25 %. Nevertheless, for $L_{RPHD} \geq 3$ there is no decrease in the network lifetime because of the limited length of the reverse path length. We conclude that utilizing unidirectional links with at most two relay nodes in the reverse path leads to maximal network lifetime values and employment of unidirectional links that necessitate reverse paths with more than two relay nodes does not provide any lifetime gains.

If the unidirectionality level of the links are low, the maximum possible network lifetime can be achieved by employing less than two relay nodes in the reverse path. Furthermore, the level of unidirectionality can change as a function of time, especially in extreme conditions. Therefore, the decision on the maximum allowed reverse path length should also be made dynamically. Since the sink is the ultimate destination for data flows and it has significantly higher energy and computing resources than the sensor nodes, decisions on the maximum reverse path length is the responsibility of the sink. However, to make such decisions efficiently, the sink should collect information on network connectivity and channel states which can be achieved without creating significant control traffic overhead (*e.g.*, control information can be piggybacked on data packets). Furthermore, the sink can disseminate the control decisions to the sensor nodes by using the ACK packets (*i.e.*, the ACK packet content can be modified to include information on L_{RPHD} which will not be larger than a few Bytes). Note that each sensor node can be reached by the sink through ACK packets either directly or via a chain of relay nodes.

REFERENCES

[1] K. Akkaya and M. Younis, "A survey on routing protocols for wireless sensor networks," *Ad Hoc Networks*, vol. 3, pp. 325–349, 2005.

[2] V. Ramasubramanian and D. Mosse, "BRA: a bidirectional routing abstraction for asymmetric mobile ad hoc networks," *IEEE/ACM Transactions on Networking*, vol. 16, pp. 116–129, 2008.

[3] L. Sang, A. Arora, and H. Zhang, "On link asymmetry and one-way estimation in wireless sensor networks," *ACM Transactions on Sensor Networks*, vol. 6, pp. 12:1–12:25, 2010.

[4] G. Wang, D. Turgut, L. Boloni, Y. Ji, and D. C. Marinescu, "A MAC layer protocol for wireless networks with asymmetric links," *Ad Hoc Networks*, vol. 6, pp. 424–440, 2008.

[5] C. A. Boano, J. Brown, Z. He, U. Roedig, and T. Voigt, "Low-power radio communication in industrial outdoor deployments: The impact of weather conditions and ATEX-compliance," in *Proceedings of the International Conference on Sensor Networks Applications, Experimentation and Logistics (SENSAPPEAL)*, 2009, pp. 159–176.

[6] C. A. Boano, H. Wennerström, M. A. Zúñiga, J. Brown, C. Keppitiyagama, F. J. Oppermann, U. Roedig, L.-Å. Nordén, T. Voigt, and K. Römer, "Hot Packets: A systematic evaluation of the effect of temperature on low power wireless transceivers," in *Proceedings of the ACM Extreme Conference on Communication (ExtremeCom)*, 2013, pp. 7–12.

[7] V. Gungor, B. Lu, and G. Hancke, "Opportunities and challenges of wireless sensor networks in smart grid," *Industrial Electronics, IEEE Transactions on*, vol. 57, pp. 3557–3564, 2010.

[8] M. A. Zúñiga, I. Irzynska, J.-H. Hauer, T. Voigt, C. A. Boano, and K. Römer, "Link quality ranking: Getting the best out of unreliable links," in *Proceedings of the IEEE International Conference on Distributed Computing in Sensor Systems (DCOSS)*, 2011, pp. 1–8.

[9] B. B. Chen, S. Hao, M. Zhang, M. C. Chan, and A. L. Ananda, "DEAL: discover and exploit asymmetric links in dense wireless sensor networks," in *Proceedings of the IEEE Conference on Sensor, Mesh and Ad Hoc Communications and Networks (SECON)*, 2009, pp. 1–9.

[10] M. K. Marina and S. R. Das, "Routing performance in the presence of unidirectional links in multihop wireless networks," in *Proceedings of the ACM International Symposium on Mobile Ad Hoc Networking and Computing (MOBIHOC)*, 2002, pp. 12–23.

[11] J. G. Jetcheva and D. B. Johnson, "Routing characteristics of ad hoc networks with unidirectional links," *Ad Hoc Networks*, vol. 4, pp. 303–325, 2006.

[12] M. Gerla, Y.-Z. Lee, J.-S. Park, and Y. Yi, "On demand multicast routing with unidirectional links," in *Proceedings of the IEEE Wireless Communications and Networking Conference (WCNC)*, vol. 4, 2005, pp. 2162–2167.

[13] C.-H. Lin, B.-H. Liu, H.-Y. Yang, C.-Y. Kao, and M.-J. Tsai, "Virtual-coordinate-based delivery-guaranteed routing protocol in wireless sensor networks with unidirectional links," in *Proceedings of the IEEE International Conference on Computer Communications (INFOCOM)*, 2008, pp. 351–355.

[14] S. Mank, R. Karnapke, and J. Nolte, "MLMAC-UL and ECTS-MAC – two MAC protocols for wireless sensor networks with unidirectional links," in *Proceedings of the International Conference on Sensor Technologies and Applications (SENSORCOMM)*, 2009, pp. 623–629.

[15] S. T. Ozyer, B. Tavli, K. Dursun, and M. Koyuncu, "Systematic investigation of the effects of unidirectional links on the lifetime of wireless sensor networks," *Computer Standards & Interfaces*, vol. 36, pp. 132–142, 2013.

[16] J. Yick, B. Mukherjee, and D. Ghosal, "Wireless sensor network survey," *Computer Networks*, vol. 52, pp. 2292–2330, 2008.

[17] F. Ishmanov, A. S. Malik, and S. M. Kim, "Energy consumption balancing (ECB) issues and mechanisms in wireless sensor networks (WSNs): a comprehensive overview," *European Transactions on Telecommunications*, vol. 22, pp. 151–167, 2011.

[18] A. Gogu, D. Nace, A. Dilo, and N. Meratnia, "Review of optimization problems in wireless sensor networks," in *Telecommunications Networks - Current Status and Future Trends*, J. Hamilton Ortiz, Ed. InTech, 2012, pp. 153–180.

[19] M. Rahimi, R. Baer, O. Iroezi, J. Garcia, J. Warrior, D. Estrin, and M.Srivastava, "Cyclops: in situ image sensing and interpretation in wireless sensor networks," in *Proceedings of the ACM Conference on Embedded Networked Sensor Systems (SenSys)*, 2005, pp. 192–204.

[20] W. Heinzelman, A. Chandrakasan, and H. Balakrishnan, "An application specific protocol architecture for wireless microsensor networks," *IEEE Transactions on Wireless Communications*, vol. 1, pp. 660–670, 2002.

[21] B. Tavli and W. Heinzelman, "Energy-efficient real-time multicast routing in mobile ad hoc networks," *IEEE Transactions on Computers*, vol. 60, pp. 707–722, 2011.

[22] Y. Liu, E. V. Matthiesen, and H.-P. Schwefel, "Localized algorithms for virtual backbone formation in wireless multi-hop networks with unidirectional links," in *Proceedings of the IST Mobile and Wireless Communications Summit*, 2007, pp. 1–5.

[23] Z. Cheng, M. Perillo, and W. B. Heinzelman, "General network lifetime and cost models for evaluating sensor network deployment strategies," *IEEE Transactions on Mobile Computing*, vol. 7, pp. 484–497, 2008.

[24] K. Bicakci, H. Gultekin, and B. Tavli, "The impact of one-time energy costs on network lifetime in wireless sensor networks," *IEEE Communications Letters*, vol. 13, pp. 905–907, 2009.

[25] (2014) General Algebraic Modeling System (GAMS). [Online]. Available: http://www.gams.com/

[26] G. Anastasi, M. Conti, A. Falchi, E. Gregori, and A. Passarella, "Performance measurements of motes sensor networks," in *Proceedings of the ACM Conference on Modeling, Analysis and Simulation of Wireless and Mobile Systems (MSWiM)*, 2004, pp. 174–181.

[27] E. Specht. (2014) The best known packings of equal circles in the unit circle. [Online]. Available: http://hydra.nat.uni-magdeburg.de/packing/